

# Modeling Social Group Communication with Multi-Agent Imitation Learning

Navyata Sanghvi  
Carnegie Mellon University  
Pittsburgh, PA, USA

Ryo Yonetani\*  
Carnegie Mellon University  
Pittsburgh, PA, USA

Kris M. Kitani  
Carnegie Mellon University  
Pittsburgh, PA, USA

**Abstract**—In crowded social scenarios with a myriad of external stimuli, human brains exhibit a natural ability to filter out irrelevant information and narrowly focus their attention. In the midst of multiple groups of people, humans use such *sensory gating* to effectively further their own group’s interactional goals. In this work, we consider the design of a policy network to model multi-group multi-person communication. Our policy takes as input the state of the world such as an agent’s gaze direction, body pose of other agents or history of past actions, and outputs an optimal action such as speaking, listening or responding (communication modes). Inspired by humans’ natural neurobiological filtering process, a central component of our policy network design is an information gating function, termed the *Kinesic-Proxemic-Message Gate (KPM-Gate)*, that models the ability of an agent to selectively gather information from specific neighboring agents. The degree of influence of a neighbor is based on dynamic non-verbal cues such as body motion, head pose (kinesics) and interpersonal space (proxemics). We further show that the KPM-Gate can be used to discover social groups using its natural interpretation as a social attention mechanism. We pose the communication policy learning problem as a multi-agent imitation learning problem. We learn a single policy shared by all agents under the assumption of a decentralized Markov decision process. We term our policy network as the *Multi-Agent Group Discovery and Communication Mode Network (MAGDAM network)*, as it learns social group structure in addition to the dynamics of group communication. Our experimental validation on both synthetic and real world data shows that our model is able to both discover social group structure and learn an accurate multi-agent communication policy.

## I. INTRODUCTION

We consider the design of an agent policy for modeling social group interaction within a social environment of multiple agents and multiple groups. The development of such models is important for understanding human to human interaction as well as the development of artificial intelligence systems that must interact with groups of people. When we consider multi-agent and multi-group communication scenarios, it is important to correctly model the manner in which agents receive and transmit information.

Consider a crowded party like the one in Figure 1. We will use this example to highlight important attributes needed to build a holistic multi-agent multi-group communication model.

**(1) Information Gating:** When we engage in communication with other people at a party, a large part of our communication is non-verbal. In the context of group communication, kinesics



Fig. 1: Crowded Party: Multi-agent multi-group interaction.

factors such as body motion, head pose and gestures are used to define our group membership (*i.e.*, we look at and gesture to the people we are communicating with). Proxemic factors define our interpersonal space (*e.g.*, we stand close to the people we want to communicate with). Kinesic and proxemic factors are also used to gate or constrain the transmission of information during social communication (*e.g.*, we avoid looking at or being near certain people if we do not want to communicate with them). Based on this observation, our first requirement is to design a model of multi-agent communication that explicitly models this gating mechanism based on non-verbal cues.

**(2) History of Self-Actions:** A party-goer’s actions will be influenced by her *own past* actions in conversation (*e.g.*, whether she has been speaking long and would like to yield to another, or whether she is bored and sees someone else she would rather converse with). Based on this observation, our second requirement is to design a model of multi-agent communication that explicitly encodes the past history of the agent herself.

**(3) Dynamic Number of Agents:** A party is a highly dynamic situation, where attendees join or leave the party and move about the room engaging in conversation or leaving groups when bored. As such, the *set of people* influencing this party-goer’s actions will be constantly changing as she and others move between groups, and the *degree of such influence* will also be constantly evolving throughout the conversation. Based on this observation, our third requirement is to design a model of multi-agent communication that is agnostic to the number of agents or groups.

Keeping in mind these three attributes of a holistic multi-agent multi-group interaction model, we propose the *Multi-Agent Group Discovery and Communication Mode (MAG-*

\*Ryo Yonetani is currently at OMRON SINIC X, Tokyo, Japan

*DAM) Network* . The MAGDAM network is a deep neural network which consists of (1) a NEIGHBOR GATING MODULE that implements a gating function to select the most relevant information from specific neighbor agents; (2) a SELF-STATE ENCODER which encodes the agents past actions; and (3) FUSION MODULE which combines the output of the Neighbor Gating Module and Self-State Encoder to predict the next agent action. To enable reasoning over a dynamic number of agents, we make two modeling assumptions. (1) We assume that the choice of actions for each of the agents are a decentralized process so that each agent selects an action based on the same MAGDAM network. (2) We use a weighted pooling operation in the Neighbor Gating Module and assume that all transmitted social signals are aggregated in to a single signal.

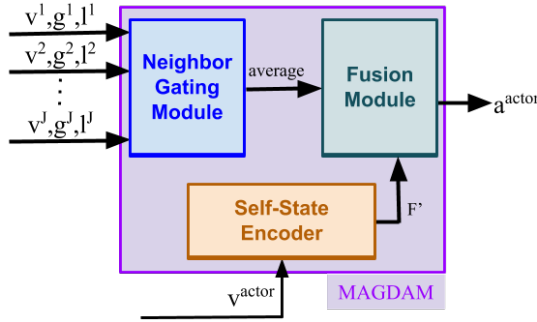


Fig. 2: Components of the MAGDAM Network: Neighbor Gating Module, Self-State Encoder and Fusion Module

The core conceptual contribution of our work is the proposal of the *Kinesic-Proxemic-Message Gate (KPM-Gate)* which is contained inside the Neighbor Gating Module. The KPM-Gate provides a gating mechanism to weigh a neighbor’s transmitted information according to the *degree of their influence* on the agent’s actions. We also show how the KPM-Gate can be used to discover social groups, *i.e.*, the set of neighbor agents most likely to be in the same group at a given time are the ones with high degrees of influence on each other’s actions (Figure 3).

Our choice of employing a gating mechanism in multi-group multi-agent communication modelling is inspired the neurobiological process of *sensory gating* exhibited in people [11] [15]. Sensory gating is the ability of filtering out unnecessary or irrelevant external stimuli. The cocktail party effect [4] is an example of sensory gating. While this example specifically demonstrates the focusing of auditory attention while ignoring other conversations (*e.g.*, at a party), similar gating is observed in the other senses to prevent the overwhelming of primary cortical areas [29][17][8]. Using our KPM-Gate, we mimic this phenomenon when considering the importance of neighbor agents’ non-verbal communications. While there exists, separately, previous work on small-group conversational dynamics [16], as well as on group detection [18], [27], [28], [32], we are the first to present a model which simultaneously (1) effectively designs multi-group multi-agent

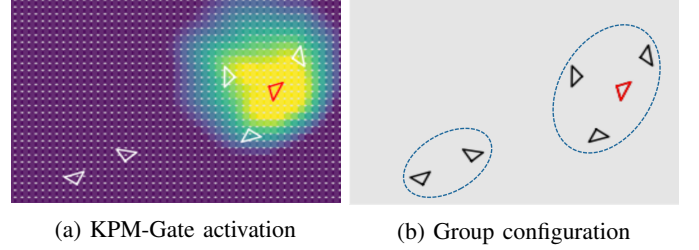


Fig. 3: **Kinesic-Proxemic-Message Gating.** Given poses, gaze directions, and communication modes of multiple parties (triangles in (a) and (b)), the KPM-Gate learns to select relevant messages.

communication protocols and which (2) gives an automatic way to discover groups implicitly as a by-product of the training process, performing comparably to state-of-the-art methods.

**Related Work:** Extensive surveys on how to adopt machine learning approaches for modeling multi-agent communication are presented in [5], [30]. Recent work makes the use of deep reinforcement learning or imitation learning to discover policies which allow agents to communicate with each other, *e.g.*, [13], [14], [21], [23], [25], [31], [24]. To the best of our knowledge, our work is the first to show how the modeling of physically constrained observations helps to learn accurate communication policies, while simultaneously giving a natural way to infer social grouping in multi-group scenarios.

Another topic closely related to our work is the analysis of human group communications, which has long been studied in multiple domains including HCI, psychology, robotics, and computer vision. As for the task of communication group discovery, state-of-the-art methods [18], [27], [28], [32] used in our experiments typically assume that group of people satisfy particular spatial layouts called F-formation [19] and discover groups of people by making use of some heuristics about how the F-formation is physically configured. By contrast, our work attempts to automatically infer group structure while performing comparably to those methods.



Fig. 4: Images of interacting agents organized into several groups - the Coffee Break (left) and Cocktail Party (right) datasets.

## II. PROBLEM FORMULATION

In the presence of multiple groups of multiple interacting agents (like in Figure 4), our goals are (1) to learn a policy of

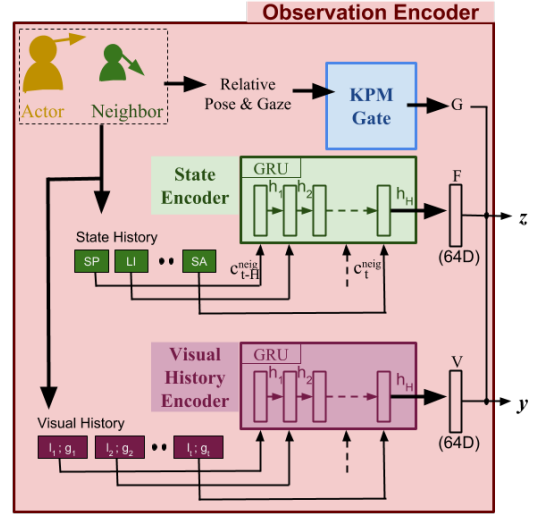
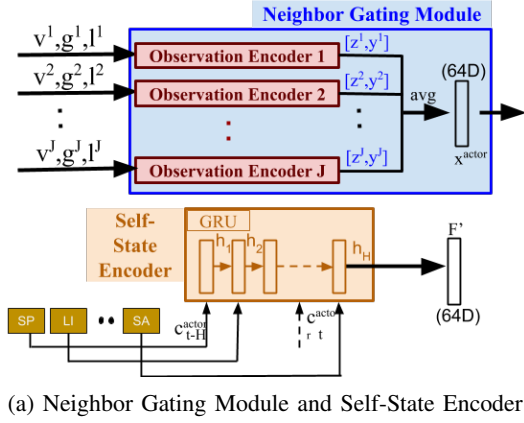


Fig. 5: (a) Observations of pose, gaze, and self state history are converted by the **Neighbor Gating Module** and **Self-State Encoder** to inputs for the Fusion Module ( $x^{actor}$  and  $F'$ ). (b) The **Observation Encoder** within the Neighbor Gating Module learns to score relevance ( $G$ ) of encoded observations of neighbor state history ( $F$ ) and visual history ( $V$ ).

social interaction for each agent and (2) discover social group structure that guide that social interaction. Consider again the cocktail party scene in Figure 1. We leverage the observation that, in such social settings, each participant visually notices the relative positions and gaze directions of other people in their field of view, based on which the participant decides whether or not the observed person’s state information is relevant to advancing communication within their own group. Using this information and their own state of activity, the participant chooses to take an action to advance intra-group communication.

To formalize the sequential decision process of multi-agent multi-group communication, we pose the process as a Decentralized Markov Decision Process (Dec-MDP) [3], [2]. Multi-group communications proceed as follows: (1) each agent observes a part of the current state of the environment (*i.e.*, observes the state of nearby agents), (2) the agent takes an action based on the observation, and (3) the agents’ joint action induces a state transition of the environment and they receive a latent reward.

The Dec-MDP for  $N$  socially interacting agents over a time period of length  $T$  is defined by a tuple  $\mathbb{D} = \langle \mathcal{S}, \mathcal{U}, P, R, \Omega, O \rangle$ .  $\mathcal{S}$  is the agents’ set of joint states. In our problem, each agent’s state consists of (1) its current communication action, and (2) its group assignment. We define set  $\Phi^m = \{1, \dots, B\}$ , as a set of  $B$  groups that agent  $A^m$  may be assigned to. Thus,  $\phi_t^m \in \Phi^m$  is a particular assignment at time step  $t$  during interaction,  $\forall m \in \{1, \dots, N\}$ ,  $\forall t \in \{1, \dots, T\}$ .  $\mathcal{U}$  is the agents’ set of joint actions. The same set of communication actions  $U$  is available to each agent, so that  $\mathcal{U} = U^N$ .  $P$  is the joint state transition function under a joint action.  $R$  is the reward function on transition under a joint

action.  $\Omega$  is the agents’ set of joint observations. The same set of observations  $Z$  is available to each agent, so  $\Omega = Z^N$ .

In our problem, at each step  $t \in \{1, \dots, T\}$ , each agent observes (1) a subset of other agents’ communication action histories, (2) this subset’s kinesic and proxemic information, and (3) their own communication action history.  $O$  is the observation function on transition under a joint action. Joint full observability: all agents’ observations together determine the joint state. Clearly, this is true if an agent’s observed kinesic and proxemic information can be mapped to its group assignment.

Thus we attempt to learn a decentralized policy  $\pi$  shared by all agents. For each agent, this maps its observations  $Z$  into actions  $U$ . To ensure joint full observability, agents must implicitly learn group assignments  $\phi$  from visually observed information while learning  $\pi$ . These group assignments induce a non-injective and non-surjective mapping of  $N$  agents into  $B$  groups, *i.e.*, multiple agents may be mapped into one group during a demonstration, while some groups may remain agentless.

Considering the requirements of the dynamic situation described in Section I, we note the following: Formulating our policy prediction in a decentralized way has the advantage of (1) being efficiently parallelizable, and (2) allowing for variation in the number of agents. Furthermore, group assignments are implicitly learned using our gating mechanism, described subsequently. This has the advantage of (1) allowing variations in an agent’s group assignment, and (2) not requiring a fixed, pre-determined set of influencing neighbor agents. Our next section provides architectural details of our network and our approach to solving the problem via multi-agent imitation learning.

### III. GROUP COMMUNICATION POLICY NETWORK

Keeping in mind insights into human social interaction and natural sensory gating detailed in Section I, we design a deep MAGDAM network to model multi-group multi-agent communication. As described in the preceding two sections, we recognize the need of a decentralized multi-group multi-agent communication model to contain the following components: (1) an encoding of the agent's observations of its neighbor's attitude and actions, (2) an encoding of the agent's observations of the self, and (3) a decision-making module that maps these learned internal representations to the agent's next best action. Toward this goal, we first describe our MAGDAM network, and then our multi-agent imitation learning approach.

#### A. The MAGDAM Network

As shown in Figure 2, the MAGDAM network consists of three modules: (a) *Neighbor Gating Module*: This module aggregates observations from surrounding agents in the environment into an internal encoding; (b) *Self-State Encoder Module*: This encodes the agent's own state history, i.e., its communication action history; (c) *Fusion Module*: This module decides the agent's next action based on the agent's encoded observations of its neighbors and of itself. Specifically, it incorporates the outputs of the Neighbor Gating Module and Self-state Encoder and generates a probability vector over the next action of the agent.

1) *Neighbor Gating Module*: This module aggregates encoded observations of surrounding agents' actions and non-verbal communications into an internal representation. Specifically, it consists of  $J$  *Observation Encoders* for the  $J$  nearest-neighbor agents, as shown in Figure 5(a).

**OBSERVATION ENCODERS:** The Neighbor Gating Module computes a weighted information encoding for each neighbor, using *Observation Encoders*. Each Observation Encoder performs sensory gating for the agent under consideration  $A^m$  with respect to its neighbor  $A^{n_i}$ 's actions and non-verbal communications ( $i \in \{1, \dots, J\}$ ). The Observation Encoder, consists of three components (Figure 5(b)).

(1) **KPM-Gate:** The Kinesic-Proxemic-Message Gate (KPM-Gate) takes agent  $A^m$ 's current physical observations (e.g., gaze, pose, inter-personal distance, etc.) of its neighbor agent  $A^{n_i}$  in order to compute a gating weight. The gating weight can be interpreted as the importance assigned to  $A^{n_i}$ 's state and non-verbal communications in deciding  $A^m$ 's next action. At time  $t$ , let  $A^m$  have gaze direction  $\mathbf{g}_t^m \in \mathbb{R}^2$  and absolute position  $\mathbf{l}_t^m \in \mathbb{R}^2$ . Let neighbor  $A^{n_i}$  have gaze direction  $\mathbf{g}_t^{n_i} \in \mathbb{R}^2$  and absolute position  $\mathbf{l}_t^{n_i} \in \mathbb{R}^2$ , where  $i \in \{1, \dots, J\}$ . In our implementation, inputs to the KPM-Gate are relative gaze direction  $\mathbf{g}_t^{(n_i \leftarrow m)}$  and relative rotated position  $\mathbf{l}_t^{(n_i \leftarrow m)}$  of  $A^{n_i}$  w.r.t.  $A^m$ :

$$\mathbf{g}_t^{(n_i \leftarrow m)} = R(\phi) \mathbf{g}_t^{n_i} \quad (1)$$

$$\mathbf{l}_t^{(n_i \leftarrow m)} = R(\phi)(\mathbf{l}_t^{n_i} - \mathbf{l}_t^m) \quad (2)$$

where  $R(\phi)$  is the rotation matrix associated with angle  $\phi = \frac{\pi}{2} - \arctan(\mathbf{g}_t^m)$  (rad). The KPM-Gate  $G(\mathbf{g}_t^{(n_i \leftarrow m)}, \mathbf{l}_t^{(n_i \leftarrow m)})$

is a two-layer perceptron. Its inputs (1) and (2) are first concatenated and fed into a fully-connected layer with a 64-dimensional output activated by an exponential linear unit (ELU) [7]. This is followed by another fully-connected layer with a one-dimensional output activated by a hard-sigmoid function [9]. This allows our KPM-Gate to output an 'importance' score  $G \in [0, 1]$ .

(2) **State Encoder:** This encodes  $A^m$ 's observations of its neighbor  $A^{n_i}$ 's past states. Let the history horizon length under consideration be  $H$ . The state of  $A^{n_i}$  at time-step  $t$  is its communication mode, represented by a  $|U|$ -dimensional one-hot vector  $\mathbf{c}_t^{n_i}$ , a dimension for each possible mode. The neighbor's state history, serving as input to the State Encoder is then:

$$\mathbf{v}_t^{n_i} = [\mathbf{c}_{t-H+1}^{n_i}, \dots, \mathbf{c}_t^{n_i}] \in \{1, 0\}^{|U| \times H} \quad (3)$$

(3) **Visual History Encoder:** This encodes  $A^m$ 's observations of its neighbor  $A^{n_i}$ 's physical, non-verbal communication history (e.g., gaze, pose, inter-personal distance, etc.). In our implementation, the neighbor's visual history is composed of its relative rotated position and gaze history, which serves as input to the Visual History Encoder:

$$\mathbf{p}_t^{n_i} = \begin{bmatrix} \mathbf{g}_{t-T+1}^{(n_i \leftarrow m)} & \cdot & \cdot & \cdot & \mathbf{g}_t^{(n_i \leftarrow m)} \\ \mathbf{l}_{t-T+1}^{(n_i \leftarrow m)} & \cdot & \cdot & \cdot & \mathbf{l}_t^{(n_i \leftarrow m)} \end{bmatrix}_{4 \times T}$$

As shown in Figure 5(b), the State Encoder  $F(\mathbf{v}_t^{n_i})$  and Visual History Encoder  $V(\mathbf{p}_t^{n_i})$  are each a linearly-activated gated recurrent unit (GRU) [6] with a 64-dimensional output. Each encoder learns the associated temporal dynamics and outputs neighbor 'messages'  $F \in \mathbb{R}^{64}$  and  $V \in \mathbb{R}^{64}$ . These messages are concatenated and weighted by the KPM gate's importance score to obtain the Observation Encoder output  $\mathbf{x}_t^{(n_i \leftarrow m)} \in \mathbb{R}^{128}$ :

$$\begin{aligned} \mathbf{x}_t^{(n_i \leftarrow m)} &= [\mathbf{y}_t^{(n_i \leftarrow m)}, \mathbf{z}_t^{(n_i \leftarrow m)}] \\ &= G(\mathbf{g}_t^{(n_i \leftarrow m)}, \mathbf{l}_t^{(n_i \leftarrow m)}) \cdot [F(\mathbf{v}_t^{n_i}), V(\mathbf{p}_t^{n_i})] \end{aligned} \quad (4)$$

Similar to [31], we employ average pooling of the weighted messages from each neighbor. For agent  $A^m$  and its neighbors  $A^{n_i} \in \mathcal{N}^m$  where  $|\mathcal{N}^m| = J$ , the Neighbor Gating Module outputs the average  $\mathbf{x}_t^m \in \mathbb{R}^{128}$  (Figure 5(a)):

$$\mathbf{x}_t^m = \frac{1}{J} \sum_{\{n_i : A^{n_i} \in \mathcal{N}^m\}} \mathbf{x}_t^{(n_i \leftarrow m)} \quad (5)$$

2) *Self-state Encoder*: This module transforms an agent's observations of its own past actions into an internal encoding. The Self-State Encoder takes as input the agent  $A^m$  state history. For horizon length  $H$ , the input is:

$$\mathbf{v}_t^m = [\mathbf{c}_{t-H+1}^m, \dots, \mathbf{c}_t^m] \in \{1, 0\}^{|U| \times H} \quad (6)$$

As shown in Figure 5(a), the Self-State Encoder  $F'(\mathbf{v}_t^m)$  has one layer. The input (6) is passed through a linearly-activated GRU with a 64-dimensional output, giving a self-state 'message'  $F' \in \mathbb{R}^{64}$ .

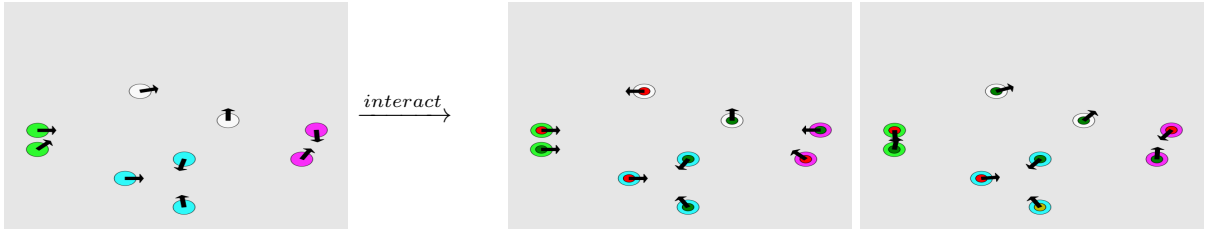


Fig. 6: **Example physical layout** [10] and subsequent mode evolution. Large circles’ colors represent group indices (agents in white have no other group members). Small circles’ colors indicate communication mode - red for speaking, yellow for distracted, green for listening. Arrows represent gaze directions.

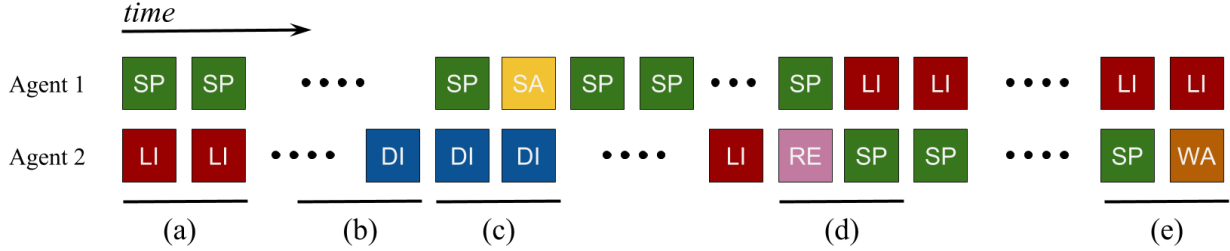


Fig. 7: **Examples of simulated communications** (static two agent case). SP: Speaking, LI: Listening, DI: Distracted, SA: Strongly Addressing, WA: Weakly Addressing, RE: Responding.

3) *Fusion Module*: This module decides the agent’s next action based on the agent’s encoded observations of its neighbors and of itself. This takes as input the concatenated outputs  $[\mathbf{x}_t^m; F'(\mathbf{v}_t^m)]$  from the Neighbor Gating Module and the Self-State Encoder (Figures 2 and 5(a)). The Fusion Module  $\pi([\mathbf{x}_t^m; F'(\mathbf{v}_t^m)])$  has two layers. The input is first fed into a fully-connected layer with a 64-dimensional output activated by an ELU. This is followed by another fully-connected layer with a  $|U|$ -dimensional output activated by a soft-max function. This output vector is thus a probability distribution over the agent  $A^m$ ’s next action from among the communication modes.

### B. Imitation Learning

By modeling the MAGDAM Network’s modules  $G$ ,  $F$ ,  $V$ ,  $F'$ , and  $\pi$  as fully-differentiable functions, we ensure that it is trainable end-to-end via back-propagation, using demonstrations of states and actions. In other words, we perform imitation learning to learn the policy  $\pi$  from several ‘expert’ demonstrations. We denote a collection of  $K$  demonstrations by  $\mathcal{D} = \{D_1 \dots, D_K\}$ , where

$$D_k = ((\mathbf{s}_{k,1}, \mathbf{u}_{k,1}), \dots, (\mathbf{s}_{k,L}, \mathbf{u}_{k,L})), \quad \forall k \in \{1, \dots, K\}$$

Here,  $L$  is the length of each trajectory  $D_k$ , and  $\mathbf{s}_{k,t}$  and  $\mathbf{u}_{k,t}$  respectively denote the state and the joint action of the agents at time step  $t$  in demonstration  $k$ . In this work, we adopt the approach of behavior cloning, which learns  $\pi$  from  $\mathcal{D}$  directly, via supervised learning *without needing to explicitly learn state transitions or reward functions*. Similar approaches can be found in recent work on multi-agent behavior prediction [1], [26].

From Section II, recall that agent  $A^m$ ’s group assignment at time step  $t$  in demonstration  $k$  is  $\phi_{k,t}^m \in \Phi_k^m$ . However, it

is often unrealistic to obtain  $\phi_{k,t}^m$  as a part of demonstrations in the imitation learning setting. Consider a practical scenario where demonstrations are collected by recording people using a camera [10], [26], [33]. The number of people within the range of visibility of the camera may vary over time. Moreover, participants’ group assignments may vary while they dynamically interact with various groups. Such dynamic situations make it impractical to fully annotate  $\phi_{k,t}^m$  for all  $k$  and  $t$ .

Identifying and working alongside this practical limitation, we emphasize that training of the MAGDAM Network requires *no supervision with respect to group assignments*. Moreover, we discover these assignments implicitly using the KPM-Gate module  $G$ . In order to minimize the error between predicted action  $\tilde{u}_{k,t}^m \in \tilde{\mathbf{u}}_{k,t}$  and observed action  $u_{k,t}^m \in \mathbf{u}_{k,t}$ , for every agent  $A^m$ , KPM-Gate  $G$  must implicitly learn physical constraints based on non-verbal inter-agent communication. The higher the relevance score assigned by  $G$  to a neighbor agent’s encoded state and visual history, the more likely the neighbor is to be in the same group as the agent  $A^m$  under consideration, and the greater its influence on  $A^m$ ’s resulting policy  $\pi$ .

## IV. EXPERIMENTS WITH SIMULATED SOCIAL AGENTS

We aim to learn the role of kinesics and proxemics in group formation and communication policies in multi-group multi-agent scenarios through imitation learning. However, to the best of our knowledge, there are no public datasets of large-scale demonstrations of the physical positions, gaze directions, group assignments, and communication modes of multiple socially interacting people. Existing datasets [10], [26], [33] only provide sequences of the physical positions, gaze directions and group assignments (but annotated only

TABLE I: **Action prediction performance** (mean average precision) and **test loss: static agents case**,  $H = 15$ 

Model (mAP's)	$J = 2$	4	8	12	Model (losses)	$J = 2$	4	8	12
Other States Only (OSO)	0.67	0.69	0.70	0.68	Other States Only (OSO)	0.99	0.95	0.89	1.00
Self States Only (SSO)	0.76	0.76	0.76	0.76	Self States Only (SSO)	0.29	0.29	0.29	0.29
Average Pooling (AveP)	0.87	0.86	0.85	0.85	Average Pooling (AveP)	0.21	0.22	0.22	0.22
Social Pooling (SocP)	0.85	0.84	0.84	0.84	Social Pooling (SocP)	0.21	0.22	0.22	0.25
<b>MAGDAM Network</b>	<b>0.88</b>	<b>0.88</b>	<b>0.89</b>	<b>0.88</b>	<b>MAGDAM Network</b>	<b>0.20</b>	<b>0.21</b>	<b>0.20</b>	<b>0.21</b>

 TABLE II: **Action prediction performance** (mean average precision) and **test loss: dynamic agents case**,  $H = 15$ 

Model (mAP's)	$J = 2$	4	8	12	Model (losses)	$J = 2$	4	8	12
Other States Only (OSO)	0.57	0.62	0.65	0.64	Other States Only (OSO)	1.24	1.12	1.05	1.07+
Self States Only (SSO)	0.78	0.78	0.78	0.78	Self States Only (SSO)	0.31	0.31	0.31	0.31
Average Pooling (AveP)	0.85	0.86	0.85	0.85	Average Pooling (AveP)	0.26	0.26	0.25	0.25
Social Pooling (SocP)	0.85	0.85	0.86	0.85	Social Pooling (SocP)	0.27	0.27	0.25	0.26
<b>MAGDAM Network</b>	<b>0.87</b>	<b>0.87</b>	<b>0.88</b>	<b>0.88</b>	<b>MAGDAM Network</b>	<b>0.25</b>	<b>0.23</b>	<b>0.25</b>	<b>0.22</b>

sparsely). More importantly, *no communication mode annotations are provided*. To evaluate our approach, we simulate realistic multi-group communication based on prior studies on the protocol of group communications [16]. Our simulated scenarios focus on sequences of non-verbal interactions while the physical layout of agents are based on real-world datasets cited above.

**Initial Agent Layout Data:** We experiment with both artificially constructed and real-world data to form our initial multi-group layouts - specifically, we use (a) Synthetic [10]<sup>1</sup>, (b) Coffee Break [10], and (c) Cocktail Party [33] datasets to provide 100, 120, and 320 non-identical and independent agent layouts respectively, of multiple people (from 6 to 12 in each layout) organized into several groups (Figure 4). We reiterate that group assignment information is used only for the ground truth and *not* for supervisory training signals to the MAGDAM network. Instead our MAGDAM network, infers group assignment information through the use of the KPM gating function.

**Interaction Episodes:** To design communication protocols, we refer to a study on multimodal small-group conversational dynamics [16]. Using a set of designed conversational rules, we roll out 600-step interaction episodes starting from each set of initial layouts ((a),(b) and (c) above) to obtain three sets of training data. Figure 6 gives an example of an initial multi-group layout and subsequent mode evolution.

**Rules of Interaction:** We summarize our designed rules for both **static** and **dynamic** scenarios. The static scenario consists of agents who stay within a social group and do not transition to other groups. The dynamic scenario consists of agents who transition from group to group, leading to a temporal evolution of group assignments through an episode. We hypothesize that our automatic KPM gating mechanism will learn to discover relevant neighbors in both static and dynamic scenarios.

In the static scenario, agents take one of the following modes: **Speaking, Listening, Distracted, Strongly Addressing, Weakly Addressing, Responding**. In the dynamic scenario, a 7th mode, **Moving**, is added. In the static scenario, as shown in Fig. 7(a), one agent in each group is Speaking while

the others are Listening. Listening agents change their mode to Distracted (Fig. 7(b)) with a certain probability. After some time steps, Speaking agents can change their mode to Strongly Addressing, to draw back the attention other agents if any other group member is Distracted (Fig. 7(c)). An agent can also transition to Weakly Addressing (Fig. 7(e)). Once a Speaking agent has spoken for some time, it will yield to another. The next identified speaker is then simulated to be Responding followed by Speaking (Fig. 7(d)). For agents who do not belong to any group (as shown with no color in Figure 6), they are simulated to act as if they are communicating with an agent outside the scene. In the dynamic scenario, a group member who is Distracted may choose to start Moving toward another group. Any time a Moving agent joins a new group, it is identified as the next speaker.

We now describe experiments and results of applying the MAGDAM network to predict the communication modes of simulated social agents.

**Baselines:** We compare the MAGDAM network with the following baselines, including communication models used in prior work:

a) *Other-States-Only (OSO)*: We omit self-state encoder  $F'$  from the MAGDAM network to use communication dependence on neighbor observations alone. This baseline model will help us understand whether observations of the self are sufficient for modeling social interaction.

b) *Self-State-Only (SSO)*: We omit the Neighbor Module from the MAGDAM network to use communication dependence on self state alone. This baseline model will help us understand whether observations of nearby agents are sufficient for modeling social interaction.

c) *Average Pooling (AveP)*: Prior work studies the role of message broadcasting from one agent to all agents [13], [24] or particular neighbors [31] by average pooling such messages. We implement this message broadcasting baseline by omitting the KPM-Gate  $G$  from the MAGDAM network so that all neighbor encoded ‘messages’  $F$  and  $V$  are equally relevant. Eqn. (4) is then  $\mathbf{x}_t^{(n_i \leftarrow m)} = [F(\mathbf{v}_t^{n_i}) \ V(\mathbf{v}_t^{n_i})]$ . This baseline model will help us understand if the equal weighting of messages from nearby agents is optimal for modeling social interaction.

<sup>1</sup><http://profs.sci.univr.it/~cristanm/ssp/>

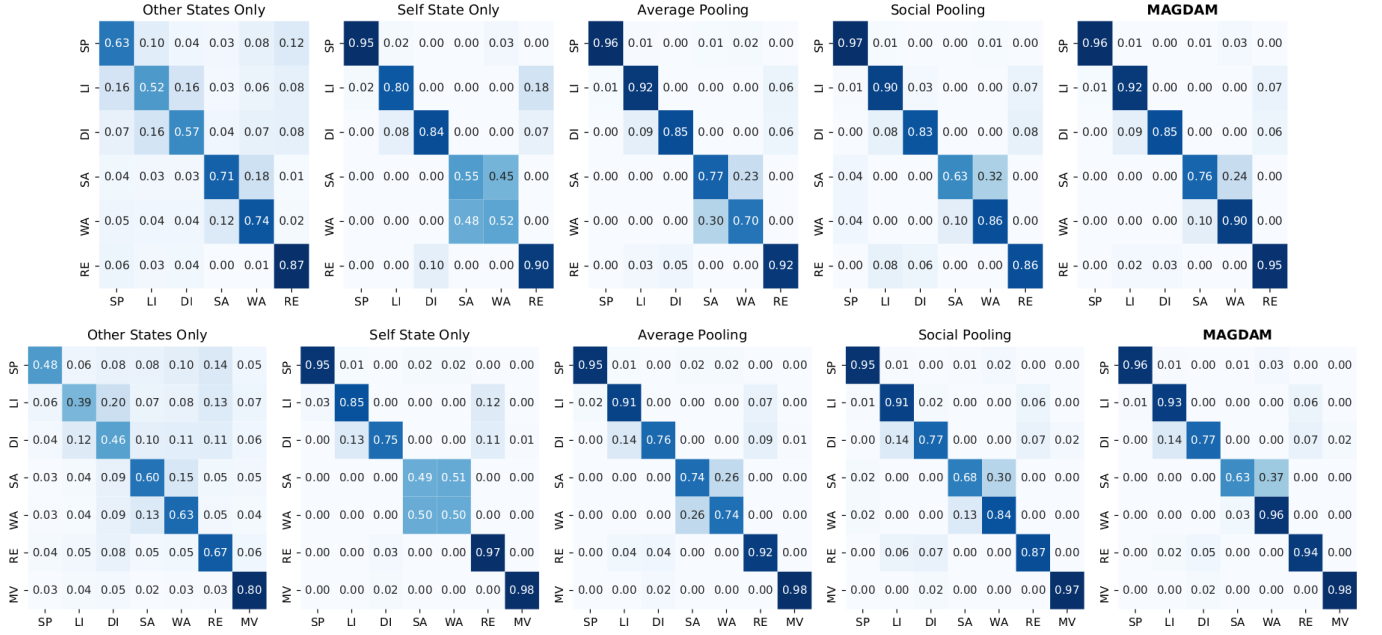


Fig. 8: **Confusion matrices on action prediction:** Top ( $6 \times 6$ ) - Static agents case. Bottom ( $7 \times 7$ ) - Dynamic agents case. SP: Speaking, LI: Listening, DI: Distracted, SA: Strong Addressing, WA: Weak Addressing, RE: Responding, MV: Moving.

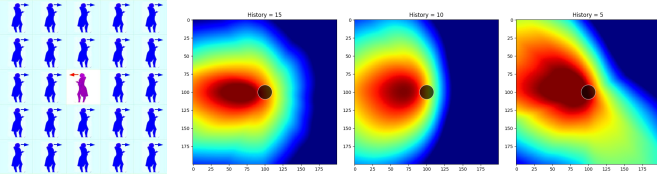


Fig. 9: **Learned Gating from Non-Verbal Cues:** Across different history windows  $H \in \{15, 10, 5\}$ , given a target agent  $A^m$  (left panel: magenta figure, right panels: black circles) in the center of the image, warmer colors indicate higher outputs from gating function  $G$  at varying neighbor agent  $A^{n_i}$  positions (left panel: blue figures) in a fine grid around  $A^m$ , when  $A^m$  and  $A^{n_i}$ 's gaze directions are along  $-x$ -axis and  $+x$ -axis respectively.

*d) Social Pooling (SocP):* We adopt social pooling [1], [22] as a second message broadcasting baseline. The social pooling model uses a grid that divides the 2D physical world into non-overlapping regions and pools messages by regions. In our implementation, we use a  $4 \times 4$  grid around target locations, each of size  $50 \times 50$  pixels. For each region, we average  $x_t^{(n_i \leftarrow m)}$  over neighbors  $A^{n_i}$  located in that region. For this baseline, the Neighbour Module of MAGDAM is replaced by a concatenation operator that simply concatenates the pooled messages over the grid. We expect this baseline to learn to gate messages by learning a static weighting over the grid.

**Training/Evaluation Scheme:** Demonstrations of multi-group communication were simulated as described previously. For each layout in each dataset (Synthetic, Coffee Break and Cock-

tail Party), agents changed modes 600 times, *i.e.*,  $K = 100$  or 120 or 320,  $L = 600$ . We split demonstrations into two subsets, and learned models on one subset to test the other. For example, when training on Coffee Break data, each subset was of 60 demonstrations each. All models were trained for 30 epochs with mini-batches of size 4096 and a history window  $H = 15$ , and we confirmed that neither further training nor smaller mini-batches improved performance. Each network was trained to minimize categorical cross entropy loss between predicted and actual actions  $\tilde{u}_{k,t}^{(n)}, u_{k,t}^{(n)}$  via Adam [20].

We report the cross-entropy loss on testing subsets. As every model predicts six (static case) or seven (dynamic case) actions in the form of discrete labels, we also evaluate model effectiveness based on mean average precision (mAP) over actions. These scores are averaged over the two test subsets.

**Results:** Tables I and II shows all model performances in communication action prediction, with a horizon length of 15, and various numbers of neighbors  $J$ . We emphasize that  $J$  is only fixed during training; since a single Observation Encoder is learned, *any* number of neighbor agents may be considered for an agent at test time - in fact, *different* numbers of neighbor agents may be considered for each agent in the scene.

As hypothesized, MAGDAM effectively learns protocols in both static and dynamic scenarios, outperforming strong baselines in terms of both mean average precision (mAP) and test loss, validating our choices of various encoding modules and demonstrating each one's necessity. While these are results of training on the Synthetic Dataset, results on other datasets show similar trends and are presented in Section VI.

Figure 8 describes the confusion matrices of action prediction for all networks with history window  $H = 15$  and number

TABLE III: **Performance on group detection:** F1 scores under the  $|G|$  criterion.

DS [18], HVFF-ms [27], GCFF [28], and GRUPO [32] compared against KPM-Gate (trained using various data and conditions: static and dynamic rollouts, starting from synthetic and real-world initial layouts)

Method→ Dataset ↓	DS	HVFF-ms	GCFF	GRUPO	KPM-Gate					
					Static Rollout			Dynamic Rollout		
					Synthetic	Coffee Break	Cocktail Party	Synthetic	Coffee Break	Cocktail Party
Synthetic	0.74	0.73	<b>0.91</b>	N/A	0.96	0.96	<b>0.99</b>	0.98	<b>0.99</b>	0.93
Coffee Break	0.39	0.30	<b>0.63</b>	N/A	<b>0.63</b>	0.61	0.60	<b>0.60</b>	0.58	0.54
Cocktail Party	N/A	0.39	<b>0.64</b>	<b>0.64</b>	0.57	<b>0.59</b>	0.56	0.57	<b>0.59</b>	0.55

of neighbor agents considered  $J = 12$ . We confirm that OSO and SSO work complementarily: OSO predicts better if agents make strong or weak addressing decisions by observing others. On the other hand, SSO performs better when observation of the self is necessary, *i.e.*, in order to predict if agents keep speaking, listening, are distracted or responding. MAGDAM outperforms baselines for most modes, both in the static and dynamic case, with lower ambiguity.

**Learned Gating:** Figure 9 represents physical constraints learned by the MAGDAM Network’s KPM-Gate  $G$  to judge if neighbor agent  $A^{n_i}$  is in the same group as agent  $A^m$ . These visuals are obtained after training on static rollouts from the synthetic dataset initial layouts. We visualize the output from  $G$  at locations around  $A^m$  while fixing relative gaze  $g^{(n_i \leftarrow m)}$ . As expected, we see improved learning with larger history windows  $H$ , and choose  $H = 15$  in our experiments. Also as expected, we see a higher output from our KPM-Gate when agents are looking toward each other, *i.e.*, when the neighbor  $A^{n_i}$  is toward the left of the image, looking in  $+x$  direction, *i.e.*, toward  $A^m$ , who is looking in  $-x$  direction.

## V. EXPERIMENTS WITH GROUP DISCOVERY IN REAL DATA

We have demonstrated the effectiveness of the MAGDAM network in learning group communication policy with simulated social agents. We now test the effectiveness of our learned automatic sensory gating mechanism, the KPM-Gate, in discovering communication groups in real-world data [10] [33]. We test the KPM-Gate of networks trained under a variety of conditions: in either static or dynamic scenarios, from initial layouts of the Synthetic [10], Coffee Break [10] or Cocktail Party [33] datasets, each of which have several continuous frames with various numbers of people annotated with their positions, gaze directions, and group assignments (Figure 4). This gives us a *total of 6 learned KPM-Gates* to assess.

For each frame, we define a distance  $D(m, n_i)$  between two people  $A^m, A^{n_i}$  based on the output of learned gating function  $G$ :  $D(m, n_i) = 1 - \frac{1}{2}(G(g^{(n_i \leftarrow m)}, l^{(n_i \leftarrow m)}) + G(g^{(m \leftarrow n_i)}, l^{(m \leftarrow n_i)}))$  and run the DBSCAN clustering algorithm [12] to cluster people into several communication groups. Under each of the 6 condition sets described in the preceding paragraph, the MAGDAM Network was trained for 20 epochs, setting  $J = 12$ , which is sufficiently larger than group membership (6 people at most) in the datasets.

Group detection performance is measured by the F1 score under the  $|G|$  condition [10], [27]. For each frame, a group is

judged to be detected correctly if all the constituent people are grouped into a single cluster. F1 scores are then computed and averaged over frames. Several state-of-the-art group detection methods [18], [27], [28], [32] are chosen as baselines. As reported in Table III, our approach (KPM-Gate) outperforms all state-of-the-art methods on the Synthetic dataset, under both static and dynamic rollout scenarios, while performing comparably on the other two datasets (best performances in bold). This result supports our hypothesis of the necessity and efficacy of explicit sensory gating while learning group communication, and, furthermore, indicates that the physical constraints learned by MAGDAM using simulated social agents are consistent with real-world human communications.

## VI. ADDITIONAL EXPERIMENTAL ANALYSIS

Lastly, we present additional experiments and discussion regarding the behavior of our network and baselines under various conditions.

### A. Varying History Window $H$

In Tables IV and V, we present results of training our networks with various history windows  $H \in \{10, 5, 1\}$ , using static and dynamic rollouts from the synthetic dataset initial layouts. As expected, lowering the history window size lowers performance of all networks, but MAGDAM either outperforms all baselines, or performs comparably to our strongest baseline Social Pooling.

The strong performance of Social Pooling is due to the explicit spatial integration of neighbor information in a grid around the agent of interest, resulting in the implicit learning of sensory gating. Note that Social Pooling and Average Pooling networks have no data left out in their inputs - they each get the same data as our proposed network, since relative gaze and pose history is included in their visual history encoding. Furthermore, Social Pooling is made stronger by spatial binning instead of naive overall averaging. While our network must learn to appropriately weight each neighbor for pooling, Social Pooling may instead achieve the learning of attention by learning weighting over the grid. Moreover, propagating each grid’s pooled messages forward results in a higher preservation of information than in our network.

As expected, this advantage is visible in results at lower history window sizes in the static agent case, when it becomes harder to correctly learn neighbor weighting (Table IV, Figure 9). However, when neighbors are dynamic (Table V), MAGDAM still outperforms all baselines, even at lower history windows. This is because the explicit sensory gating

TABLE IV: Action prediction performance (mean average precision): static agents case,  $H = 10, 5, 1$ 

Model (mAP's, $H = 10$ )	$J = 2$	4	8	12
Other States Only (OSO)	0.65	0.68	0.66	0.65
Self States Only (SSO)	0.72	0.72	0.72	0.72
Average Pooling (AveP)	0.85	0.85	0.83	0.83
Social Pooling (SocP)	0.85	0.85	0.84	0.83
<b>MAGDAM Network</b>	<b>0.87</b>	<b>0.88</b>	<b>0.86</b>	<b>0.85</b>

Model (mAP's, $H = 5$ )	$J = 2$	4	8	12
Other States Only (OSO)	0.59	0.60	0.60	0.59
Self States Only (SSO)	0.59	0.59	0.59	0.59
Average Pooling (AveP)	0.80	0.79	0.76	0.76
Social Pooling (SocP)	<b>0.80</b>	<b>0.80</b>	<b>0.80</b>	0.79
<b>MAGDAM Network</b>	0.79	<b>0.80</b>	<b>0.80</b>	<b>0.80</b>

Model (mAP's, $H = 1$ )	$J = 2$	4	8	12
Other States Only (OSO)	0.48	0.48	0.49	0.47
Self States Only (SSO)	0.49	0.49	0.49	0.49
Average Pooling (AveP)	0.64	0.63	0.62	0.60
Social Pooling (SocP)	<b>0.69</b>	<b>0.70</b>	<b>0.69</b>	<b>0.69</b>
<b>MAGDAM Network</b>	0.68	0.68	0.67	0.66

 TABLE V: Action prediction performance (mean average precision): dynamic agents case,  $H = 10, 5, 1$ 

Model (mAP's, $H = 10$ )	$J = 2$	4	8	12
Other States Only (OSO)	0.55	0.58	0.62	0.62
Self States Only (SSO)	0.73	0.73	0.73	0.73
Average Pooling (AveP)	0.82	0.83	0.82	0.81
Social Pooling (SocP)	0.82	0.83	0.83	0.83
<b>MAGDAM Network</b>	<b>0.83</b>	<b>0.85</b>	<b>0.85</b>	<b>0.86</b>

Model (mAP's, $H = 5$ )	$J = 2$	4	8	12
Other States Only (OSO)	0.50	0.55	0.58	0.58
Self States Only (SSO)	0.63	0.63	0.63	0.63
Average Pooling (AveP)	0.75	0.75	0.74	0.75
Social Pooling (SocP)	<b>0.76</b>	0.77	0.78	0.78
<b>MAGDAM Network</b>	<b>0.76</b>	<b>0.78</b>	<b>0.79</b>	<b>0.79</b>

Model (mAP's, $H = 1$ )	$J = 2$	4	8	12
Other States Only (OSO)	0.37	0.41	0.44	0.43
Self States Only (SSO)	0.55	0.55	0.55	0.55
Average Pooling (AveP)	0.62	0.62	0.61	0.61
Social Pooling (SocP)	0.63	0.64	0.64	0.64
<b>MAGDAM Network</b>	<b>0.64</b>	<b>0.65</b>	<b>0.66</b>	<b>0.66</b>

 TABLE VI: Action prediction performance (mean average precision): static agents case,  $H = 15$ , Coffee Break [10] and Cocktail Party [33] initial layouts

Model (mAP's, Coffee Break)	$J = 2$	4	8	12
Other States Only (OSO)	0.71	0.72	0.71	0.70
Self States Only (SSO)	0.75	0.75	0.75	0.75
Average Pooling (AveP)	0.89	0.88	0.87	0.86
Social Pooling (SocP)	<b>0.91</b>	<b>0.92</b>	<b>0.91</b>	<b>0.91</b>
<b>MAGDAM Network</b>	0.90	0.91	<b>0.91</b>	<b>0.91</b>

Model (mAP's, Cocktail Party)	$J = 2$	4	8	12
Other States Only (OSO)	0.72	0.79	0.79	0.79
Self States Only (SSO)	0.73	0.73	0.73	0.73
Average Pooling (AveP)	0.91	0.94	0.94	0.94
Social Pooling (SocP)	<b>0.92</b>	<b>0.95</b>	0.94	0.94
<b>MAGDAM Network</b>	<b>0.92</b>	<b>0.95</b>	<b>0.95</b>	<b>0.95</b>

 TABLE VII: Action prediction performance (mean average precision): dynamic agents case,  $H = 15$ , Coffee Break [10] and Cocktail Party [33] initial layouts

Model (mAP's, Coffee Break)	$J = 2$	4	8	12
Other States Only (OSO)	0.60	0.65	0.68	0.68
Self States Only (SSO)	0.78	0.78	0.78	0.78
Average Pooling (AveP)	0.86	0.87	0.87	0.86
Social Pooling (SocP)	0.86	0.87	0.87	0.87
<b>MAGDAM Network</b>	<b>0.87</b>	<b>0.88</b>	<b>0.89</b>	<b>0.89</b>

Model (mAP's, Cocktail Party)	$J = 2$	4	8	12
Other States Only (OSO)	0.59	0.73	0.75	0.74
Self States Only (SSO)	0.78	0.78	0.78	0.78
Average Pooling (AveP)	0.89	0.91	0.91	0.91
Social Pooling (SocP)	0.87	0.90	0.90	0.90
<b>MAGDAM Network</b>	<b>0.89</b>	<b>0.92</b>	<b>0.93</b>	<b>0.92</b>

required to infer when to pay attention to a moving agent is advantageous over a static weighting learned over a grid, as in Social Pooling.

Further, we analyze the effect of varying number of grids in Social Pooling, at history  $H = 15$ . Results in Figure 10 show that MAGDAM outperforms Social Pooling even with larger numbers of grids under the mean average precision metric, while performing similarly under the accuracy metric. Further, MAGDAM furnishes us with a natural way to infer group membership in real-world data (Section V), which Social Pooling does not.

### B. Varying Initial Layouts (Synthetic/Coffee Break/Cocktail)

In Tables I and II, we presented results using datasets generated from synthetic data initial layouts. In Tables VI and VII we present performance results using datasets generated from real-world initial layouts in Coffee Break [10] and Cocktail Party [33] datasets. As expected, MAGDAM outperforms all baselines in the dynamic case, while performing comparably to Social Pooling in the static case. This comparison has been discussed in the previous subsection.

### C. Learned Gating Outputs

We visualize outputs of the KPM-Gate for an agent  $A^m$  at various surrounding locations of a neighbor agent  $A^{n_i}$  while

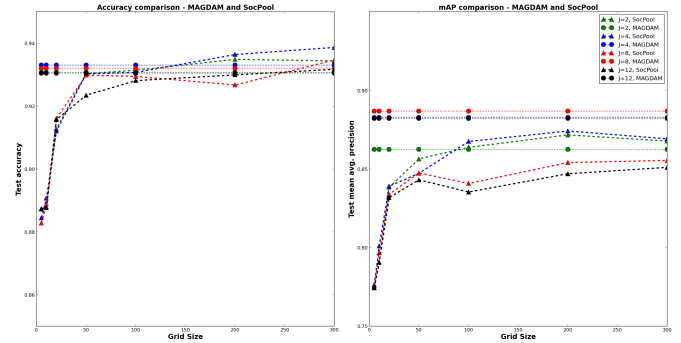


Fig. 10: Change in Social Pooling performance with varying grid size, history window  $H = 15$ . MAGDAM performs similarly to SocP under the accuracy metric, and outperforms SocP under the mean average precision metric, even with larger grid sizes.

fixing relative gaze direction. We do so for all cases of initial layout source (Synthetic, Coffee Break or Cocktail Party) and conditions (static or dynamic agents) in Figure 11. Similar to Figure 9, here, the black circles represent  $A^m$  looking in the  $-x$ -direction.  $A^{n_i}$  is assumed to be looking in the

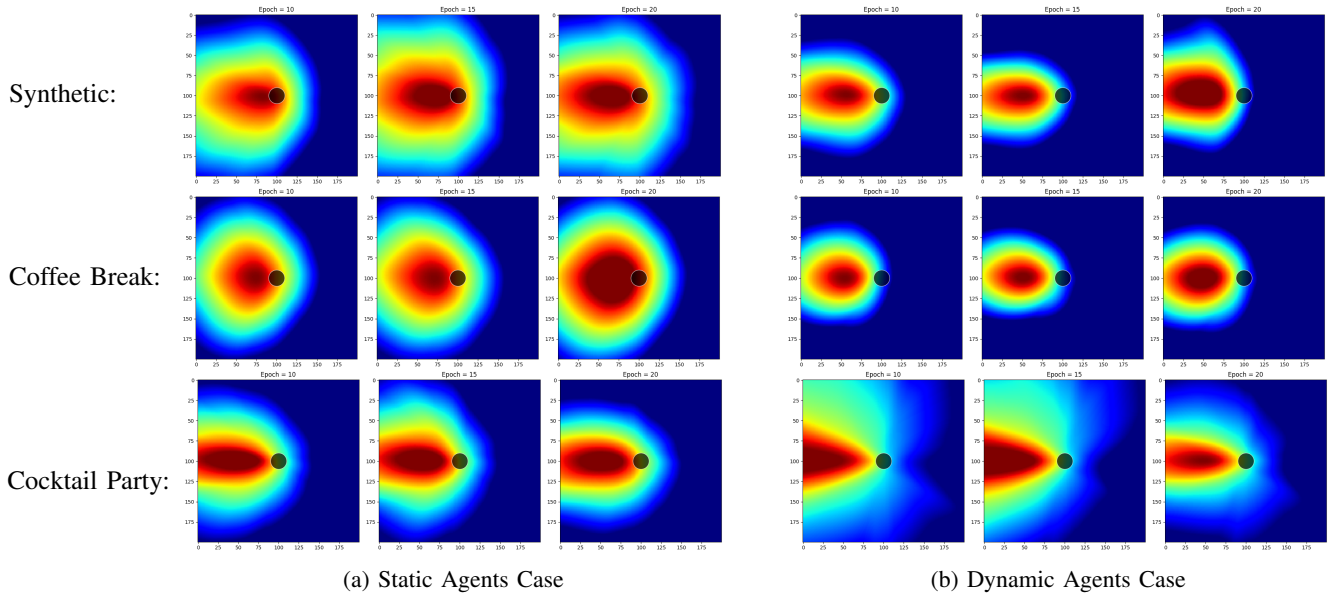


Fig. 11: **Learned gating output for static agents (left) and dynamic agents (right) cases for Synthetic, Coffee Break and Cocktail Party initial layouts, respectively. Each are displayed at training epochs 10, 15 and 20.**

$+x$ -direction. Warmer colors indicate higher outputs from the gating function at those corresponding positions of  $A^{n_i}$ .

As described in Section V, such outputs are used to infer group membership of a neighbor agent  $A^{n_i}$  with respect to the agent under consideration  $A^m$ . As can be seen in Figure 11, our network learns appropriate gating in all cases by the 20<sup>th</sup> epoch of training. Despite variations between the learned gating under various conditions, the distance function  $D(m, n_i)$  learned for clustering is informative and leads to group detection performance comparable to state-of-the-art methods (Table III).

## VII. CONCLUSION

We have presented a model of multi-group visual communications for simultaneously discovering groups and learning communication policies, based on physically constrained observations. A possible extension is to extract rewards of communications via inverse reinforcement learning. This will help us reason about communication modes, positions, and gaze directions that agents prefer under different communication contexts, *i.e.*, cooperative, competitive, *etc.* Also interesting future work would be to first gather, and then train the network with real annotated data, leading to a deeper understanding of how humans truly communicate under multi-group scenarios.

## REFERENCES

- [1] A. Alahi, K. Goel, V. Ramanathan, A. Robicquet, L. Fei-Fei, and S. Savarese. Social lstm: Human trajectory prediction in crowded spaces. In *Proceeding of the IEEE Conference on Computer Vision and Pattern Recognition*, 2016.
- [2] R. Becker, S. Zilberstein, and V. Lesser. Decentralized markov decision processes with event-driven interactions. In *Proceedings of the Third International Joint Conference on Autonomous Agents and Multiagent Systems-Volume 1*, pages 302–309. IEEE Computer Society, 2004.
- [3] D. S. Bernstein, R. Givan, N. Immerman, and S. Zilberstein. The complexity of decentralized control of markov decision processes. *Mathematics of operations research*, 27(4):819–840, 2002.
- [4] A. W. Bronckhorst. The cocktail party phenomenon: A review of research on speech intelligibility in multiple-talker conditions. *Acta Acustica united with Acustica*, 86(1):117–128, 2000.
- [5] L. Busoni, R. Babuška, and B. D. Schutter. A comprehensive survey of multiagent reinforcement learning. *IEEE Transactions on Systems, Man, and Cybernetics, Part C (Applications and Reviews)*, 38(2):156–172, March 2008.
- [6] J. Chung, Ç. Gülçehre, K. Cho, and Y. Bengio. Empirical evaluation of gated recurrent neural networks on sequence modeling. *CoRR*, abs/1412.3555, 2014.
- [7] D. Clevert, T. Unterthiner, and S. Hochreiter. Fast and accurate deep network learning by exponential linear units (elus). *CoRR*, abs/1511.07289, 2015.
- [8] F. L. Colino, G. Buckingham, D. T. Cheng, P. van Donkelaar, and G. Binsted. Tactile gating in a reaching and grasping task. *Physiological reports*, 2(3), 2014.
- [9] M. Courbariaux and Y. Bengio. Binarynet: Training deep neural networks with weights and activations constrained to +1 or -1. *CoRR*, abs/1602.02830, 2016.
- [10] M. Cristani, L. Bazzani, G. Paggetti, A. Fossati, D. Tosato, A. D. Bue, G. Menegaz, and V. Murino. Social interaction discovery by statistical analysis of f-formations. In *British Machine Vision Conference*, pages 23.1–23.12, 2011.
- [11] H. C. Cromwell, R. P. Mears, L. Wan, and N. N. Boutros. Sensory gating: a translational effort from basic to clinical science. *Clinical EEG and Neuroscience*, 39(2):69–72, 2008.
- [12] M. Ester, H.-P. Kriegel, J. Sander, and X. Xu. A density-based algorithm for discovering clusters a density-based algorithm for discovering clusters in large spatial databases with noise. In *Proceedings of the International Conference on Knowledge Discovery and Data Mining*, pages 226–231, 1996.
- [13] J. Foerster, Y. M. Assael, N. de Freitas, and S. Whiteson. Learning to communicate with deep multi-agent reinforcement learning. In *Proceeding of the Advances in Neural Information Processing Systems*, pages 2137–2145, 2016.
- [14] J. N. Foerster, G. Farquhar, T. Afouras, N. Nardelli, and S. Whiteson. Counterfactual multi-agent policy gradients. *CoRR*, abs/1705.08926, 2017.
- [15] R. Freedman, L. E. Adler, G. A. Gerhardt, M. Waldo, N. Baker, G. M. Rose, C. Drebing, H. Nagamoto, P. Bickford-Wimer, and R. Franks. Neurobiological studies of sensory gating in schizophrenia. *Schizophrenia bulletin*, 13(4):669–678, 1987.

- [16] D. Gatica-Perez. Analyzing group interactions in conversations: a review. In *Proceedings of the International Conference on Multisensor Fusion and Integration for Intelligent Systems*, pages 41–46, 2006.
- [17] S. Hillyard and G. Mangun. Sensory gating as a physiological mechanism for visual selective attention. *Electroencephalography and clinical neurophysiology. Supplement*, 40:61–67, 1987.
- [18] H. Hung and B. Kröse. Detecting f-formations as dominant sets. In *Proceedings of the International Conference on Multimodal Interfaces*, pages 231–238, 2011.
- [19] A. Kendon. *Conducting interaction: Pattern of behavior in focused encounter*. Cambridge University Press, 1990.
- [20] D. P. Kingma and J. Ba. Adam: A method for stochastic optimization. *CoRR*, abs/1412.6980, 2014.
- [21] H. M. Le, Y. Yue, and P. Carr. Coordinated multi-agent imitation learning. In *Proceeding of the International Conference on Machine Learning*, 2017.
- [22] N. Lee, W. Choi, P. Vernaza, C. B. Choy, P. H. S. Torr, and M. Chandraker. Desire: Distant future prediction in dynamic scenes with interacting agents. In *Proceedings of the IEEE Conference on Computer Vision and Pattern Recognition*, 2017.
- [23] R. Lowe, Y. Wu, A. Tamar, J. Harb, P. Abbeel, and I. Mordatch. Multi-agent actor-critic for mixed cooperative-competitive environments. *CoRR*, abs/1706.02275, 2017.
- [24] I. Mordatch and P. Abbeel. Emergence of grounded compositional language in multi-agent populations. *CoRR*, abs/1703.04908, 2017.
- [25] P. Peng, Q. Yuan, Y. Wen, Y. Yang, Z. Tang, H. Long, and J. Wang. Multiagent bidirectionally-coordinated nets for learning to play starcraft combat games. *CoRR*, abs/1703.10069, 2017.
- [26] A. Robicquet, A. Sadeghian, A. Alahi, and S. Savarese. Learning social etiquette: Human trajectory understanding in crowded scenes. In *Proceeding of the European Conference on Computer Vision*, pages 549–565, 2016.
- [27] F. Setti, O. Lanz, R. Ferrario, V. Murino, and M. Cristani. Multi-scale f-formation discovery for group detection. In *Proceedings of the International Conference on Image Processing*, pages 3547–3551, 2013.
- [28] F. Setti, C. Russell, C. Bassetti, and M. Cristani. F-formation detection: Individuating free-standing conversational groups in images. *PLOS ONE*, 10(5):1–26, 2015.
- [29] K. L. Shapiro, J. Caldwell, and R. E. Sorensen. Personal names and the attentional blink: A visual “cocktail party” effect. *Journal of Experimental Psychology: Human Perception and Performance*, 23(2):504, 1997.
- [30] P. Stone and M. Veloso. Multiagent systems: A survey from a machine learning perspective. *Autonomous Robots*, 8(3):345–383, Jun 2000.
- [31] S. Sukhbaatar, A. Szlam, and R. Fergus. Learning multiagent communication with backpropagation. In *Proceeding of the Advances in Neural Information Processing Systems*, pages 2244–2252, 2016.
- [32] M. Vazquez, A. Steinfeld, and S. E. Hudson. Parallel detection of conversational groups of free-standing people and tracking of their lower-body orientation. In *Proceedings of the IEEE/RSJ International Conference on Intelligent Robots and Systems*, 2015.
- [33] G. Zen, B. Lepri, E. Ricci, and O. Lanz. Space speaks: Towards socially and personality aware visual surveillance. In *Proceeding of the International Workshop on Multimodal Pervasive Video Analysis*, pages 37–42, 2010.